

# Anomalous mass enhancement in strongly-correlated quantum wells

Satoshi Okamoto<sup>1,\*</sup>

<sup>1</sup>*Materials Science and Technology Division, Oak Ridge National Laboratory, Oak Ridge, Tennessee 37831, USA*

We investigate the electronic properties of quantum wells consisting of a  $t_{2g}^1$ -electron system with strong correlations using dynamical-mean-field theory. The special focus is on the subband structure of such quantum wells. The effective mass is found to increase with increasing the bottom of the subband, i.e., decreasing the subband occupation number. This is due to the combination of Coulomb repulsion, whose effect is enhanced on surface layers, and longer-range hoppings. We discuss the implication of these results for the recent angle-resolved photoemission experiment on SrVO<sub>3</sub> thin films.

PACS numbers: 73.21.-b, 71.10.-w

Two-dimensional electron gases (2DEGs) realized in a variety of oxide interfaces have been attracting significant interests.<sup>1,2</sup> In particular, utilizing oxides with strong correlations for electronics would benefit from their rich phase behaviors.<sup>3</sup> For example, controlling the band structure of 2DEGs in transition-metal oxides has been proposed as a way to create non-cuprate high- $T_c$  superconductivity.<sup>4</sup> Yet, realizing metallic behavior in few-unit-cell thick oxides remains challenging.<sup>5,6</sup>

Two-dimensional metallic behavior in the confined geometry, i.e., quantum well (QW), has been studied for conventional metals. Reconstructed band structures or subband dispersion relations in QWs of Ag thin films have been confirmed using photoemission spectroscopy.<sup>7,8</sup> The subband dispersion relations of 2DEGs realized on the surface of a band insulator SrTiO<sub>3</sub> was also observed using angle-resolved photoemission spectroscopy (ARPES).<sup>9,10</sup> More recently, Yoshimatsu and coworkers have performed ARPES measurements on QWs in thin films of a correlated metal SrVO<sub>3</sub>.<sup>11</sup> The subband structures realized in such QWs can be explained using a simple tight-binding-type description reasonably well. However, the effective mass of such subbands was found to increase with decreasing the binding energy of the subband. Since this trend is opposite to what we expect based on the bulk behavior, i.e., the effective mass is reduced with decreasing binding energy and decreasing band occupancy, the origin of such an anomalous mass enhancement remains to be understood.

In this paper, we analyze model QWs consisting of a  $t_{2g}^1$  electron system as experimentally considered by Yoshimatsu *et al.* We employ the layer dynamical-mean-field theory (DMFT) with the exact-diagonalization impurity solver.<sup>12,13</sup> In correlated QWs, a smaller coordination number on surface layers induces larger mass enhancement than in the bulk region.<sup>14-18</sup> This brings about the anomalous subband-dependent mass enhancement; the effective mass becomes larger with decreasing subband binding energy or depopulating the subband. With the additional effect coming from the longer-range hopping, the subband dependent mass enhancement was found to increase dramatically. We argue that the anomalous mass enhancement reported for thin films of SrVO<sub>3</sub> is due to strong correlations and long-range transfer integral.

We consider the three-band Hubbard model involving  $t_{2g}$  electrons,  $H = H_{band} + \sum_{\mathbf{r}} H_{loc}(\mathbf{r})$ . The first term describes the non-interacting part of the system as

$$H_{band} = - \sum_{\tau, \sigma} \sum_{\mathbf{r}, \mathbf{r}'} t_{\mathbf{r}\mathbf{r}'}^{\tau} d_{\mathbf{r}\tau\sigma}^{\dagger} d_{\mathbf{r}'\tau\sigma}, \quad (1)$$

where  $d_{\mathbf{r}\tau\sigma}$  stands for the annihilation operator for an electron at site  $\mathbf{r}$ , orbital  $\tau$  with spin  $\sigma$ ,  $t_{\mathbf{r}\mathbf{r}'}^{\tau}$  is the hopping integral between orbital  $\tau$  at sites  $\mathbf{r}$  and  $\mathbf{r}'$ . For the orbital  $\tau = xy$ , we take the nearest neighbor hoppings  $t_{\mathbf{r}\mathbf{r}'}^{\tau} = t_{\pi}$  for  $\mathbf{r}' = \mathbf{r} \pm \hat{\mathbf{x}}(\hat{\mathbf{y}})$  and  $t_{\mathbf{r}\mathbf{r}'}^{\tau} = t_{\delta}$  for  $\mathbf{r}' = \mathbf{r} \pm \hat{\mathbf{z}}$ , and the second-neighbor hopping  $t_{\mathbf{r}\mathbf{r}'}^{\tau} = t_{\sigma'}$  for  $\mathbf{r}' = \mathbf{r} \pm \hat{\mathbf{x}} \pm \hat{\mathbf{y}}$ . Here,  $\hat{\mathbf{x}}(\hat{\mathbf{y}}, \hat{\mathbf{z}})$  is the unit vector along the  $x(y, z)$  direction. The hopping parameters for the other orbitals are given by interchanging the coordinates  $x, y$ , and  $z$  accordingly. Parameter values are taken from previous density functional theory results as  $t_{\pi} = 0.281$ ,  $t_{\delta} = 0.033$ , and  $t_{\sigma'} = 0.096$  (eV).<sup>19</sup>  $H_{loc}$  describes the local interaction as

$$H_{loc} = \frac{1}{2} \sum_{\substack{\tau, \tau', \tau'' \\ \tau''', \sigma, \sigma'}} U^{\tau\tau'\tau''\tau'''} d_{\tau\sigma}^{\dagger} d_{\tau'\sigma'}^{\dagger} d_{\tau''\sigma''} d_{\tau'''\sigma'''} - \mu \sum_{\tau, \sigma} d_{\tau\sigma}^{\dagger} d_{\tau\sigma}. \quad (2)$$

Here, the site index  $\mathbf{r}$  is suppressed for simplicity, and  $\mu$  is the chemical potential. Since we consider  $t_{2g}$  electron systems, we assume the following relation:  $U = U' + 2J$ , where  $U = U^{\tau\tau\tau\tau}$  (intraorbital Coulomb),  $U' = U^{\tau\tau'\tau'\tau}$  (interorbital Coulomb),  $J = U^{\tau\tau'\tau'\tau}$  (interorbital exchange) =  $U^{\tau\tau\tau'\tau'}$  (interorbital pair transfer) for  $\tau \neq \tau'$ , and other components are absent.<sup>20</sup> As in Ref. 11, we consider QWs in which a finite number of correlated layers stack along the  $z$  direction with the open-boundary condition and the periodic-boundary condition along the  $x$  and  $y$  directions.

Before going into the detailed analysis taking into account the correlation effects, let us first discuss the low-energy electronic behavior focusing on quasiparticle bands. For this purpose, we consider the following effective one-dimensional Schrödinger equation<sup>21</sup>

$$\left[ Z_z^{\tau} \{ \tilde{\epsilon}_{\mathbf{k}}^{\tau} - \mu + \Re \Sigma_z^{\tau}(0) \} \delta_{z, z'} + \sqrt{Z_z^{\tau} Z_{z'}^{\tau}} t_{\mathbf{k}}^{\tau} \delta_{z, z' \pm 1} \right] \varphi_{z, \mathbf{k}}^{\tau\alpha} = E_{\mathbf{k}}^{\tau\alpha} \varphi_{z, \mathbf{k}}^{\tau\alpha}, \quad (3)$$

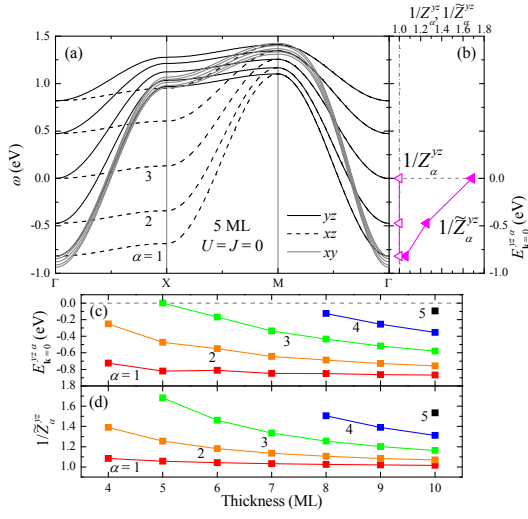


FIG. 1: (Color online) (a) Dispersion relation as a function of momentum for the non-interacting 5-ML-thick quantum well. (b) Subband quasiparticle weights  $Z_\alpha^{\tau}$  and  $\tilde{Z}_\alpha^{\tau}$  as a function of  $E_{\mathbf{k}=0}^{\tau\alpha}$ . Note that the graph is rotated by 90 degrees so that  $E_{\mathbf{k}=0}^{\tau\alpha}$  matches the the vertical axis of panel (a). (c)  $E_{\mathbf{k}=0}^{\tau\alpha}$  (binding energy at  $\mathbf{k} = 0$  times  $-1$ ) and (d) Effective quasiparticle weight  $\tilde{Z}_\alpha^{\tau}$  as a function of the thickness of the quantum well.

where  $\Sigma_z^\tau(\omega)$  is the electron self-energy at orbital  $\tau$  in layer  $z$  computed in the layer DMFT,  $Z_z^\tau$  is the layer-dependent quasiparticle weight defined by  $Z_z^\tau = \{1 - \Re \partial_\omega \Sigma_z^\tau(\omega)|_{\omega=0}\}^{-1}$ .  $\varepsilon_{\mathbf{k}}^\tau$  is the in-plane dispersion and  $t_{\mathbf{k}}^\tau$  is the out-of-plane hopping element for orbital  $\tau$  with the in-plane momentum  $\mathbf{k} = (k_x, k_y)$ . For  $\tau = yz$ , these are explicitly given by  $\varepsilon_{\mathbf{k}}^{yz} = -2t_\pi \cos k_y - 2t_{\sigma'} \cos k_x$  and  $t_{\mathbf{k}}^{yz} = -t_\pi - 2t_\delta \cos k_y$ .  $\alpha$  labels the subband with the eigenfunction  $\varphi_z^{\tau\alpha}$  in the increasing order of subband energy  $E_{\mathbf{k}}^{\tau\alpha}$ . For non-interacting systems,  $Z_z^\tau$  is always 1. As an example, the energy eigenvalue  $E_{\mathbf{k}}^{\tau\alpha}$  for 5-monolayer (ML)-thick QW is plotted in Fig. 1 (a). We notice that subbands originating from  $yz(xz)$  orbitals are not parallel, while  $xy$  subbands are. This is because the second-neighbor hopping between neighboring layers induces the  $\mathbf{k}$  dependence in out-of-plane hopping  $t_{\mathbf{k}}^{yz(xz)}$ . For orbital  $yz(xz)$ ,  $t_{\mathbf{k}}^\tau = -t_\pi - 2t_\delta \cos k_{y(x)}$  and, therefore, the subband separation becomes large when  $k_{y(x)}$  approaches 0. As a result, the Fermi velocity becomes small as if *the effective mass is enhanced* as the Fermi momentum is reduced or the subband occupation is reduced.

The low-energy electronic behaviors of correlated QWs are governed by the quasiparticle subbands. The degree of correlation effects enters as the quasiparticle weight or the mass enhancement of the subband. Using the solution of Eq. (3), the subband-dependent quasiparticle

weight is given by<sup>21,22</sup>

$$Z_\alpha^\tau = \sum_z Z_z^\tau \left| \varphi_z^{\tau\alpha} \right|_{\mathbf{k}=\mathbf{k}_F^\alpha}^2. \quad (4)$$

From Eq. (4), it is clear that the subband quasiparticle weight becomes unity in the absence of correlations, i.e.,  $Z_z^\tau = 1$  leads to  $\sum_z \left| \varphi_z^{\tau\alpha} \right|_{\mathbf{k}=\mathbf{k}_F^\alpha}^2 = 1$  (normalization of the quasiparticle eigenfunction). Another important quantity is the *effective quasiparticle weight* defined by

$$\tilde{Z}_\alpha^\tau = \left. \frac{\partial_{\mathbf{k}} E_{\mathbf{k}}^{\tau\alpha}}{\partial_{\mathbf{k}} \varepsilon_{\mathbf{k}0}^\tau} \right|_{\mathbf{k}=\mathbf{k}_F^\alpha}. \quad (5)$$

Here,  $\mathbf{k}_F^{\tau\alpha}$  is the Fermi momentum for  $\alpha$ th subband, and  $\varepsilon_{\mathbf{k}k_z}^\tau$  is the bulk dispersion. For  $\tau = yz$ , we have  $\varepsilon_{\mathbf{k}k_z}^{yz} = \varepsilon_{\mathbf{k}}^{yz} + 2t_{\mathbf{k}}^{yz} - 2t_\pi \cos k_z$ . Thus,  $\tilde{Z}_\alpha^\tau$  measures the change in the Fermi velocity with respect to its bulk value. In Ref. 11,  $\tilde{Z}_\alpha^\tau$  was used to discuss the mass enhancement.

Because of the  $\mathbf{k}$  dependence of the interlayer hopping matrix  $t_{\mathbf{k}}^\tau$ ,  $\tilde{Z}$  can be smaller than unity even without correlations. Fig. 1 (b) plots the result of  $1/\tilde{Z}$  for a non-interacting 5-ML-thick QW. The results for the thickness dependence for non-interacting QWs, the bottom of subband dispersion  $E_{\mathbf{k}=0}^{\tau\alpha}$  and  $1/\tilde{Z}_\alpha^{\tau}$ , are summarized in Figs. 1 (c) and (d). One can notice that  $1/\tilde{Z}_\alpha^{\tau}$  increases as  $E_{\mathbf{k}=0}^{\tau\alpha}$  approaches the Fermi level,  $\omega = 0$ . A similar trend was reported experimentally. However, the effective mass enhancement  $1/\tilde{Z}_\alpha^{\tau}$  is at most 70%. Therefore, the band effect alone does not account for the nearly 300% of mass enhancement reported in Ref. 11.

In order to see the effect of correlations rather quantitatively, here we employ the layer DMFT whose self-consistency condition is closed by<sup>14-16,21</sup>

$$G_z^\tau(\omega) = \int \frac{d^2k}{(2\pi)^2} G_{zz}^\tau(\mathbf{k}, \omega). \quad (6)$$

Here,  $G_z^\tau$  is the local Green's function on layer  $z$ , and the lattice Green's function matrix on the right hand side is given as a function of  $\mathbf{k}$  and  $z$ -axis coordinate as  $\hat{G}(\mathbf{k}, \omega) = [(\omega + \mu)\mathbf{1} - \hat{H}_{band}(\mathbf{k}) - \hat{\Sigma}(\mathbf{k}, \omega)]^{-1}$ . The hopping matrix  $\hat{H}_{band}(\mathbf{k})$  is given by an in-plane Fourier transformation of  $H_{band}$  as  $\hat{H}_{band}(\mathbf{k}) = (\varepsilon_{\mathbf{k}}^\tau \delta_{z,z'} + t_{\mathbf{k}}^\tau \delta_{z,z'\pm 1}) \delta_{\tau,\tau'}$ . In DMFT, the self-energy matrix is approximated as  $\hat{\Sigma}(\mathbf{k}, \omega) = \Sigma_z^\tau(\omega) \delta_{z,z'} \delta_{\tau,\tau'}$ . The local self-energy is obtained by solving the effective impurity model defined by the local interaction term coupling with an effective medium. In this study, we use the exact diagonalization impurity solver using the Arnoldi algorithm.<sup>23,24</sup> Here, the effective medium is approximated as a finite number of bath sites, and the impurity Hamiltonian is given by

$$H_{imp} = H_{loc} + \sum_{i,\tau,\sigma} \varepsilon_{i\tau} c_{i\tau\sigma}^\dagger c_{i\tau\sigma} + \sum_{i,\tau,\sigma} \left( v_{i\tau} c_{i\tau\sigma}^\dagger d_{\tau\sigma} + h.c. \right). \quad (7)$$

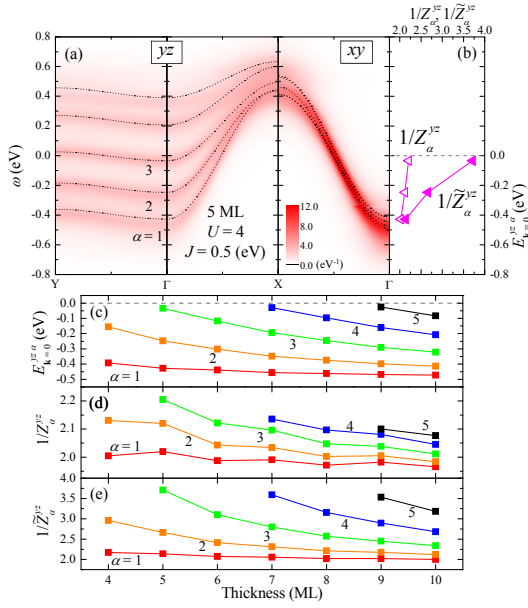


FIG. 2: (Color online) (a) Orbitaly-resolved spectral function as a function of momentum and frequency for the interacting 5-ML-thick QW. Dotted lines indicate the solution of Eq. (3),  $E_{\mathbf{k}}^{\tau\alpha}$ , obtained using the layer DMFT result of the quasiparticle weight  $Z_z^\tau$ . Note that  $yz$  and  $xz$  bands are symmetric with respect to  $X \leftrightarrow Y$ . (b) Subband quasiparticle weights  $Z_\alpha^{yz}$  and  $\tilde{Z}_\alpha^{yz}$  as a function of  $E_{\mathbf{k}=0}^{yz, \alpha}$ . Note that the graph is rotated by 90 degrees as in Fig. 1 (b). (c)  $E_{\mathbf{k}}^{yz, \alpha}$ , (d) quasiparticle weight  $Z_\alpha^{yz}$ , and (e) effective quasiparticle weight  $\tilde{Z}_\alpha^{yz}$  as a function of the thickness of QW. As the interaction strength,  $U = 4$  and  $J = 0.5$  (eV) are used.

$c_{i\tau\sigma}$  is the annihilation operator of an electron at the  $i$ th bath site with its potential  $\varepsilon_{i\tau}$  and hybridization strength with the impurity orbital  $\tau$  denoted by  $v_{i\tau}$ . Because of the exponentially growing Hilbert space with respect to the numbers of orbitals and electrons, we consider two bath sites per correlated orbital, i.e.,  $i = 1, 2$ . In our numerical simulations, we used temperature  $T = 10^{-2}$  (eV) to retain low-energy states with Boltzmann factors larger than  $10^{-6}$  and only consider paramagnetic solutions.

Figure 2 (a) shows the result of orbitaly-resolved spectral function  $A^\tau(\mathbf{k}, \omega) = -\frac{1}{\pi} \sum_z \Im G_{zz}^\tau(\mathbf{k}, \omega)$  as well as  $E_{\mathbf{k}}^{\tau\alpha}$  as dotted lines for 5-ML-thick interacting QW with  $U = 4$  and  $J = 0.5$  (eV). For  $A^\tau(\mathbf{k}, \omega)$ , the self-energy is extrapolated to the real axis using the Padé approximation.<sup>24</sup> In comparison with the non-interacting case, the band width is reduced by about 50 % due to correlations. We notice that  $E_{\mathbf{k}}^{\tau\alpha}$  reproduces the peak positions of  $A^\tau(\mathbf{k}, \omega)$  fairly well. There are 5 subbands for both  $yz$  and  $xy$ , but those in the latter are indistinguishable because all subbands are located within the range of  $2t_\delta \sim 0.07$  eV. Thus, we focus on  $yz$  subbands in the following discussion. As in Fig. 1 (b), the mass enhancements  $1/Z_\alpha^{yz}$  and  $1/\tilde{Z}_\alpha^{yz}$  are plotted in Fig. 2 (b). The bottom of subband dispersion  $E_{\mathbf{k}=0}^{yz, \alpha}$ ,  $1/Z_\alpha^{yz}$ , and  $1/\tilde{Z}_\alpha^{yz}$

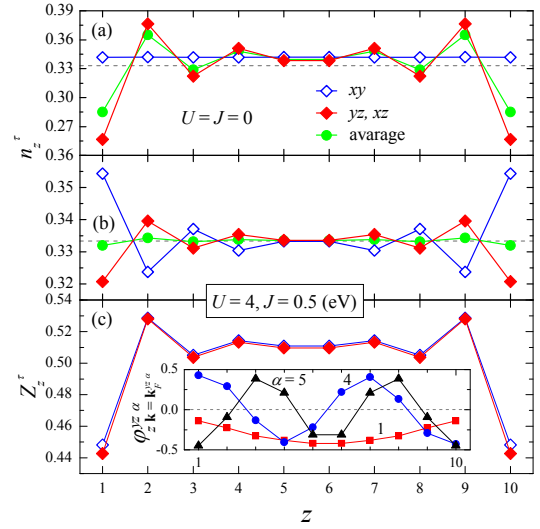


FIG. 3: (Color online) (a) Orbitaly-resolved occupation number as a function of position  $z$  for the non-interacting 10-ML-thick QW. (b) Same as (a) for the interacting model and (c) the local quasiparticle weight as a function of  $z$ . Layer DMFT with  $U = 4$  and  $J = 0.5$  (eV) is used for (b) and (c). Inset: Quasiparticle wave functions  $\varphi_z^{yz, \alpha}$  at  $\mathbf{k} = \mathbf{k}_F^{yz, \alpha}$ .

are plotted for interacting QWs with varying thicknesses in Figs. 2 (c), (d), and (e), respectively. Although  $1/Z_\alpha^{yz}$  shows an increase with increasing  $E_{\mathbf{k}=0}^{yz, \alpha}$ , it is only from  $\sim 2$  to  $\sim 2.2$ . On the other hand,  $1/\tilde{Z}_\alpha^{yz}$  shows a rather steep increase from  $\sim 2$  to  $\sim 3.8$  as reported experimentally.<sup>11</sup>

Aside from the quantitative difference, non-interacting QWs and interacting QWs behave quite similarly. As a small but clear difference, some of interacting QWs have a larger number of occupied  $yz$  subbands, 7 and 9-ML-thick QWs. This is caused by the different orbital polarization. As shown in Fig. 3 (a) and (b), non-interacting QWs have larger orbital polarization with smaller occupancy in  $yz$  and  $xz$  orbitals on surface layers compared with interacting QWs. This is because  $yz$  and  $xz$  bands have a quasi-one-dimensional character on the surface layers and their effective band width is reduced to about half of its bulk value. The average charge density also shows Friedel-type oscillatory behavior with respect to  $z$ . On the other hand, in the interacting case, the orbital polarization and the charge disproportionation are significantly suppressed. This is because, in correlated systems, the charge susceptibility is suppressed at integer fillings. This behavior was found to be insensitive to the choice of the interaction strength (not shown).

Figure 3 (c) shows the position-dependent quasiparticle weight  $Z_z^\tau$ , and its inset the quasiparticle eigenfunctions for  $yz$  electron at the Fermi level. Since an eigenfunction with larger  $\alpha$  has larger weight on the surface layers, the effective mass of such a subband is more strongly renormalized. A similar effect was discussed for Mott-insulator/band-insulator heterostruc-

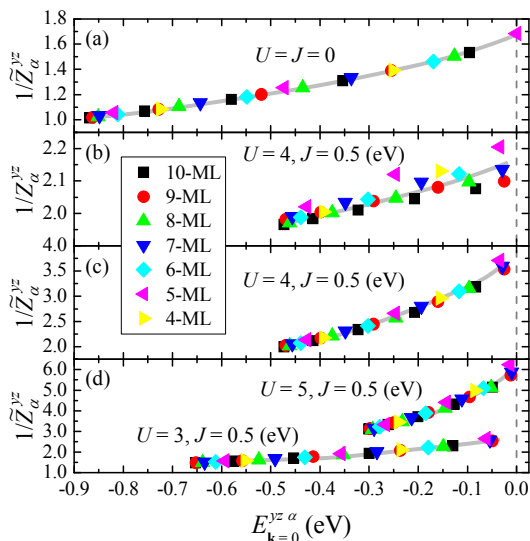


FIG. 4: (Color online) Subband mass enhancement. (a) Effective mass enhancement  $1/\tilde{Z}_\alpha^{yz}$  for the non-interacting model as a function of  $E_{\mathbf{k}=0}^{yz}$ . (b) Mass enhancement  $1/\tilde{Z}_\alpha^{yz}$  and (c)  $1/\tilde{Z}_\alpha^{yz}$  for the interacting model with  $U = 4$  and  $J = 0.5$  (eV). (d)  $1/\tilde{Z}_\alpha^{yz}$  for the interacting model with  $U = 3$ ,  $J = 0.5$  and  $U = 5$ ,  $J = 0.5$  (eV). Vertical broken lines indicate the Fermi level, and light bold lines are the guides to the eye.

tures where the central part of heterostructures shows strong mass enhancement because this region is close to a Mott insulator.<sup>21</sup> In the present case, the strong mass renormalization takes place in surface layers where the coordination number is smaller.<sup>14-18</sup> The additional enhancement in  $1/\tilde{Z}_\alpha^{yz}$  is caused by the momentum dependent inter-layer hoppings as discussed earlier.

Figure 4 summarizes the mass enhancement as a function of the bottom of the subband. The effect of the momentum dependent inter-layer hoppings is rather small for non-interacting QWs because it comes from the small hopping intensity  $t_{\sigma'}$ . The mass enhancement  $1/\tilde{Z}_\alpha^{yz}$  originating purely from the correlation effects shows rather small dependence on  $E_{\mathbf{k}=0}^{yz}$  either because the relative en-

hancement of the effective mass on surface layers is about 10 % [See Fig. 3 (c)]. On the other hand,  $1/\tilde{Z}_\alpha^{yz}$  shows strong  $E_{\mathbf{k}=0}^{yz}$  dependence because both the band effects and correlations are included. The effective mass enhancement  $1/\tilde{Z}_\alpha^{yz}$  somewhat depends on the correlation strength as shown in Fig. 4 (d). With a reasonable parameter set, the experimentally reported mass enhancement can be semiquantitatively reproduced.

We notice that the number of subbands is overestimated by  $\sim 1$  for interacting QWs compared with the experimental observation.<sup>11</sup> A possible explanation for this discrepancy is that, in the experiment of Ref. 11, the surface layer is made of  $\text{VO}_2$ , so that the symmetry and the valence state of surface V ions largely deviate from those in the bulk. Also, we cannot exclude the possibility of surface lattice relaxation by which conduction electrons are strongly localized on the surface layer. In these cases, the surface V sites would not contribute to the ARPES spectrum near the Fermi level as those in the bulk. Detailed study including these effects would be necessary to fully understand the nature of  $\text{SrVO}_3$  QWs including the dimensional crossover and the metal-insulator transition.<sup>5,11</sup>

Summarizing, we investigated the electronic properties of correlated quantum wells consisting of a  $t_{2g}^1$ -electron system using dynamical-mean-field theory. The special focus is on the subband structure of such quantum wells. The subband effective mass was found to increase with decreasing band occupancy. Such an anomalous mass enhancement has been reported for  $\text{SrVO}_3$  thin films. The present theory provides a reasonable account for this observation as the combined effect of Coulomb repulsion, whose effect is enhanced on surface layers, and longer-range hoppings.

The author thanks H. Kumigashira, K. Yoshimatsu, and A. Fujimori for valuable discussions and sharing experimental data prior to publication. The author is grateful for V. R. Cooper for discussion and C. G. Baker for his advice on coding. This work was supported by the U.S. Department of Energy, Office of Basic Energy Sciences, Materials Sciences and Engineering Division.

\* okapon@ornl.gov

<sup>1</sup> A. Ohtomo, D. A. Muller, J. L. Grazul, and H. Y. Hwang, *Nature (London)* **419**, 378 (2002).  
<sup>2</sup> A. Ohtomo and H. Y. Hwang, *Nature (London)* **427**, 423 (2004).  
<sup>3</sup> H. Takagi and H. Y. Hwang, *Science* **327**, 1601 (2010); J. Mannhart and D. G. Schlom, *Science* **327**, 1607 (2010).  
<sup>4</sup> J. Chaloupka and G. Khaliullin, *Phys. Rev. Lett.* **100**, 016404 (2008).  
<sup>5</sup> K. Yoshimatsu, T. Okabe, H. Kumigashira, S. Okamoto, S. Aizaki, A. Fujimori, and M. Oshima, *Phys. Rev. Lett.* **104**, 147601 (2010).  
<sup>6</sup> J. Liu, S. Okamoto, M. van Veenendaal, M. Kareev, B. Gray, P. Ryan, J. W. Freeland, and J. Chakhalian, *Phys.*

*Rev. B* **83**, 161102(R) (2011).  
<sup>7</sup> D. A. Evans, M. Alonso, R. Cimino, and K. Horn, *Phys. Rev. Lett.* **70**, 3483 (1993).  
<sup>8</sup> I. Matsuda, T. Ohta, and H. W. Yeom, *Phys. Rev. B* **65**, 085327 (2002).  
<sup>9</sup> A. F. Santander-Syro, O. Copie, T. Kondo, F. Fortuna, S. Pailhès, R. Weht, X. G. Qiu, F. Bertran, A. Nicolaou, A. Taleb-Ibrahimi, P. Le Fèvre, G. Herranz, M. Bibes, N. Reyren, Y. Apertet, P. Lecoeur, A. Barthélémy, and M. J. Rozenberg, *Nature (London)* **469**, 189 (2011).  
<sup>10</sup> W. Meevasana, P. D. C. King, R. H. He, S.-K. Mo, M. Hashimoto, A. Tamai, P. Songpiritthigul, F. Baumberger, and Z.-X. Shen, *Nature Mater.* **9**, 114 (2011).  
<sup>11</sup> K. Yoshimatsu, K. Horibe, H. Kumigashira, T. Yoshida,

- A. Fujimori, and M. Oshima, *Science* **333**, 319 (2011).
- <sup>12</sup> A. Georges, G. Kotliar, W. Krauth, and M. J. Rozenberg, *Rev. Mod. Phys.* **68**, 13 (1996).
- <sup>13</sup> M. Caffarel and W. Krauth, *Phys. Rev. Lett.* **72**, 1545 (1994).
- <sup>14</sup> M. Potthoff and W. Nolting, *Phys. Rev. B* **59**, 2549 (1999).
- <sup>15</sup> M. Potthoff and W. Nolting, *Phys. Rev. B* **60**, 7834 (1999).
- <sup>16</sup> S. Schwieger, M. Potthoff, and W. Nolting, *Phys. Rev. B* **67**, 165408 (2003).
- <sup>17</sup> A. Liebsch, *Phys. Rev. Lett.* **90**, 096401 (2003).
- <sup>18</sup> H. Ishida, D. Wortmann, and A. Liebsch, *Phys. Rev. B* **73**, 245421 (2006).
- <sup>19</sup> E. Pavarini, A. Yamasaki, J. Nuss, and O. K. Andersen, *N. J. Phys.* **7** 188 (2005).
- <sup>20</sup> S. Sugano, Y. Tanabe, and H. Kamimura, *Multiplets of Transition-Metal Ions in Crystals* (Academic, New York, 1970).
- <sup>21</sup> S. Okamoto and A. J. Millis, *Phys. Rev. B* **70**, 241104(R) (2004).
- <sup>22</sup> A. Rüegg, S. Pilgram, and M. Sigrist, *Phys. Rev. B* **75**, 195117 (2007).
- <sup>23</sup> R. B. Lehoucq, D. C. Sorensen, and C. Yang, *ARPACK Users' Guide* (SIAM, Philadelphia, 1997).
- <sup>24</sup> C. A. Perroni, H. Ishida, and A. Liebsch, *Phys. Rev. B* **75**, 045125 (2007).